

# Hydrothermal synthesis of ZnSe:Mn quantum dots and their optical properties

Hisaaki Nishimura,<sup>1</sup> Yuxin Lin,<sup>1</sup> Masayuki Hizume,<sup>1</sup> Taichi Taniguchi,<sup>1</sup> Naoteru Shigekawa,<sup>1</sup> Tomomi Takagi,<sup>2</sup> Susumu Sobue,<sup>2</sup> Shoichi Kawai,<sup>2</sup> Eiichi Okuno,<sup>2</sup> and  
DaeGwi Kim<sup>1,\*</sup>

<sup>1</sup> Department of Applied Physics, Graduate School of Engineering, Osaka City  
University

3-3-138, Sugimoto, Sumiyoshi-ku, Osaka 558-8585, Japan

<sup>2</sup> Advanced Research and Innovation Center, DENSO CORPORATION

500-1, Minamiyama, Komenoki-cho, Nisshin-shi, Aichi 470-0111, Japan

\*E-mail: [tegi@a-phys.eng.osaka-cu.ac.jp](mailto:tegi@a-phys.eng.osaka-cu.ac.jp)

Water-soluble Mn<sup>2+</sup>-doped ZnSe quantum dots (QDs) were synthesized using a hydrothermal method. The characteristics of the precursor solutions greatly affected the photoluminescence (PL) properties of the ZnSe:Mn QDs. In QDs synthesized with alkaline precursor solutions, a PL band originating from the intra-3*d* shell transition of Mn<sup>2+</sup> is clearly observed, indicating that Mn<sup>2+</sup> ions are thoroughly doped inside the ZnSe QDs. The PL quantum yield of the ZnSe:Mn QDs synthesized under the optimum conditions reached 20%. By introducing a ZnS shell at the surface of the ZnS:Mn QDs, the PL properties were improved and the PL quantum yield was further increased to 30%.

## I. INTRODUCTION

Solar power generation is an important renewable energy source and silicon-based solar cells are currently the most widespread type of solar cell used. In general, however, silicon solar cells have low spectral sensitivity to ultraviolet light. As a method to solve this problem, the development of a wavelength conversion material that converts light in the ultraviolet wavelength region to visible light at the high spectral sensitivity of a silicon-based solar cell is desired [1-8]. Recently, the application of organic dyes [1-5] and semiconductor quantum dots (QDs) [3,6-9] as wavelength conversion materials has attracted much attention. Because organic dyes can only absorb light in a limited wavelength range corresponding to their intrinsic absorption characteristics, the range of wavelengths that can be used in such a wavelength conversion material is also limited [3,10,11]. Conversely, semiconductor QDs can absorb light in all wavelength regions shorter than their absorption onset and it is possible to control the onset wavelength via the QD size owing to quantum size effects [12,13]. Furthermore, when compared to organic dyes, QDs are more stable against light irradiation [10,11]. Therefore, it is thought that they have great potential as a wavelength conversion material.

So far, studies on the optical properties of semiconductor QDs have primarily been conducted on Cd-chalcogenide materials, such as CdSe [14-17] and CdTe [18-21]. From the viewpoint of the application of QDs, the preparation of QDs from Cd-free materials is desired. In recent years, chalcopyrite semiconductors such as CuInS<sub>2</sub> [22,23] and AgInS<sub>2</sub> [24,25] as well as the II-VI semiconductor of ZnSe [26-28] have attracted considerable attention as promising candidates for Cd-free QDs. The absorption onset of CuInS<sub>2</sub> and AgInS<sub>2</sub> QDs is in the near-infrared to visible region, whereas the absorption onset of ZnSe QDs is in the blue to ultraviolet region. In this study, we focus on ZnSe

QDs doped with  $Mn^{2+}$  impurities (ZnSe:Mn QDs) because ZnSe absorbs light in the blue to ultraviolet region and shows orange emission due to the  $d-d$  transition in the emission center of  $Mn^{2+}$  [29-31]. Therefore, ZnSe:Mn QDs are thought to be suitable as a wavelength conversion material for improving the conversion efficiency of silicon-based solar cells.

ZnSe:Mn QDs possessing high photoluminescence (PL) quantum yield (QY) have been synthesized via the hot-injection method using chemical reactions in an organic solvent. Gan *et al.* successfully synthesized ZnSe:Mn QDs with a PL QY of 50% [30]. Zeng *et al.* reported that the PL QY reaches 60% at maximum for ZnSe:Mn/ZnS core/shell QDs [31]. In recent years, attempts have been made to apply Mn-doped semiconductor QDs having high PL QY to bioimaging [32,33]. For applications to bioimaging, water-soluble QDs are necessary. It is well known that oil-soluble QDs prepared using the hot injection method can be dispersed in water via ligand exchange [34,35]; however, the PL intensity usually decreases due to the ligand exchange. Therefore, directly synthesizing water-soluble ZnSe:Mn QDs having good optical properties is still an important subject.

Water-soluble QDs can be prepared using hydrothermal and/or reflux methods. Aboulaich *et al.* reported the synthesis of water-soluble ZnSe:Mn and ZnSe:Mn/ZnS core/shell QDs with PL QYs of 3.5% and 9%, respectively, using a reflux method [36]. Hardzei *et al.* successfully synthesized ZnSe:Mn/ZnS core/shell QDs with PL QYs of 10% using a hydrothermal method [37]. Consequently, the PL QYs of water-soluble ZnSe:Mn QDs reported so far are not very high.

In this study, we aim to improve the PL QY of water-soluble ZnSe:Mn QDs. In the hydrothermal synthesis of water-soluble QDs, the selection of the ligand greatly affects the PL properties of the QDs. We previously reported that *N*-acetyl-*L*-cysteine (NAC)-capped CdTe and ZnSe QDs have PL QYs of 60% or higher [21,38,39]. Therefore, the

optimum preparation conditions of NAC-capped ZnSe:Mn QDs were investigated by changing the synthesis conditions such as the pH of the precursor solutions, the  $Mn^{2+}$  concentration, and the Se/Zn molar ratio. We successfully prepared ZnSe:Mn QDs with a PL QY of 20% by optimizing the synthesis conditions. Furthermore, the PL QY was increased to 30% for ZnSe:Mn/ZnS core/shell QDs.

## II. EXPERIMENTS

ZnSe:Mn QDs were synthesized using a hydrothermal method [37,39]. A Zn-source,  $Zn(ClO_4)_2 \cdot 6H_2O$  (1.0 mmol), and NAC (4.8 mmol) were dissolved in 50 mL of deionized (DI) water, followed by the addition of an Mn-source,  $Mn(ClO_4)_2 \cdot 6H_2O$  (0.02 mmol), to this solution. The aqueous solution was adjusted to a pH of 8.5 via the stepwise addition of 1.0 M NaOH; then, a freshly prepared NaHSe solution (0.2 mmol) was added. Finally, the precursor solution was adjusted to a pH of 10. To deduce the optimum conditions, we prepared various precursor solutions with different molar ratios of  $Zn^{2+}$  and  $Mn^{2+}$ . The influence of the pH of the precursor solutions was also investigated. In addition, 10 mL of the precursor solution was loaded into an autoclave and incubated at 200°C for specified periods of time.

To improve the PL QY, ZnSe:Mn/ZnS core/shell QDs were synthesized. First, a ZnS precursor solution was prepared as follows.  $Zn(ClO_4)_2 \cdot 6H_2O$  (0.4 mmol) and NAC (1.92 mmol) were dissolved in 20 mL of DI water followed by an adjustment of the pH to 5. Then,  $Na_2S \cdot 9H_2O$  (0.12 mmol) was added and the precursor solution was adjusted to a pH of 6. The ZnS precursor solution was added to the already prepared ZnSe:Mn QD solution, and ZnSe:Mn/ZnS core/shell QDs were synthesized under microwave irradiation.

The crystal structures of the prepared QDs were investigated via X-ray powder

diffraction (XRD) with Cu K $\alpha$  ( $\lambda = 0.154$  nm) as the incident radiation. Transmission electron microscopy (TEM) images were obtained using a JEOL JEM-2100. For the X-ray photoelectron spectroscopy (XPS) measurements, the monolayer structure of the ZnSe:Mn and ZnSe:Mn/ZnS QDs was prepared as follows. The Si substrates were cleaned via immersion in a fresh piranha solution (1/3 (v/v) mixture of 30% H<sub>2</sub>O<sub>2</sub> and 98% H<sub>2</sub>SO<sub>4</sub>) for 20 min (*caution*: piranha solutions react violently with organic materials). The substrates were then rinsed with water and used immediately after cleaning. At the beginning of the sample preparation, an adhesion layer of polyelectrolytes of positively charged poly(diallyldimethylammonium chloride) (PDDA) was deposited to enhance the binding of the QDs. The thickness of the PDDA layer is  $\sim 0.5$  nm [40,41]. The monolayer structure of the ZnSe:Mn and ZnSe:Mn/ZnS QDs was then deposited onto the PDDA layer. A Shimadzu ESCA-3400 with a Mg K $\alpha$  (1.253 keV) source was used for XPS experiments.

The absorption and PL spectra were measured using a JASCO V-650 UV-Vis spectrophotometer and an FP-8300 spectrofluorometer, respectively. In measurements of the PL decay profiles, the third-harmonic-generation (THG) light (355 nm) of a laser-diode-pumped yttrium aluminum garnet (YAG) laser with a pulse duration of 20 ns was used as the excitation light. For the measurements in the millisecond time region, the THG-YAG laser was operated with a repetition rate of 50 Hz and the PL-decay curves were observed using a 500-MHz digitizing oscilloscope. For the measurements of the PL decay profiles in the microsecond time region, the excitation source was operated at 20 kHz and the PL-decay profiles were obtained using a time-correlated single-photon counting method.

### III. RESULTS AND DISCUSSION

In the synthesis of semiconductor QDs using a hydrothermal method, the pH of the precursor solutions is an important parameter [39,42] and the optimum pH value for the preparation of ZnSe QDs has been reported to be a pH of 6 [39]. Therefore, the ZnSe:Mn QDs were first prepared from a ZnSe:Mn (2% Mn) precursor solution with a pH of 6. Figures 1(a) and 1(b) show the absorption and PL spectra of the ZnSe and ZnSe:Mn QDs, respectively, prepared with a reaction time of 30 min using a precursor solution with a pH of 6. It is obvious that the spectra in Figs. 1(a) and 1(b) coincide. In the absorption spectrum, an absorption peak is clearly observed with higher energy than the band gap energy (2.67 eV) of a ZnSe bulk crystal, and band-edge (BE)-PL is observed to be the main PL band in the PL spectrum.

It is well known that Mn-related PL (Mn PL) originating from the intra-3*d* shell transition of Mn<sup>2+</sup> in Mn-doped II-VI semiconductors such as ZnS:Mn, CdS:Mn, and ZnSe:Mn appears near ~2.1 eV. However, in Fig. 1(b), no PL band having a peak near 2.1 eV is observed and a defect-related PL band is observed on the low energy side of BE-PL. This result suggests that Mn ions are not doped to the ZnSe QD in the synthesized ZnSe:Mn QDs.

Defect-related PL usually has a decay time of hundreds of nanoseconds to a microsecond, while Mn PL shows a slow decay in the order of milliseconds. Therefore, we measured the PL-decay profiles to confirm the possibility of Mn-doping. Figure 2 shows the PL-decay profiles detected at 2.68 eV in the ZnSe and ZnSe:Mn QDs. Both profiles are coincident and show decay in the order of a microsecond. From the above results, it is concluded that Mn ions are not doped inside the ZnSe QDs prepared from the ZnSe:Mn precursor solution with a pH of 6. Mn PL was not observed even in samples prepared at reaction times of 5 min, 10 min, and 20 min.

In previous studies, water-soluble Mn-doped QDs, such as ZnS:Mn [32,33] and

ZnSe:Mn QDs [36,37], in which Mn PL was clearly observed, have usually been synthesized from precursor solutions in the alkaline pH range. Therefore, ZnSe:Mn QDs were prepared again from alkaline precursor solutions. Figure 3 shows the absorption and PL spectra of the ZnSe:Mn QDs prepared from a ZnSe:Mn (2% Mn) precursor solution with a pH of 9. Focusing on the PL spectrum, a PL band with a peak near 2.1 eV is clearly observed, which is quite different from the result shown in Fig. 1(b).

The PL-decay profile detected at the PL peak of 2.1 eV is shown in Fig. 4. This profile is much longer than that of the defect-related PL shown in Fig. 2. The PL band has a slow decay component of  $\sim 1$  ms, which is consistent with the intrinsic nature of the intra- $3d$  transition in  $\text{Mn}^{2+}$  [29,42-45]. These results suggest that the doping of Mn ions succeeded in the ZnSe:Mn QDs prepared from the precursor solution with a pH of 9. Therefore, it is confirmed that the pH value of the precursor solution is a very important parameter in the preparation of ZnSe:Mn QDs. Compared with the absorption spectrum shown in Fig. 1, the absorption spectrum in Fig. 3 is broad. This is because that the size distribution of the ZnSe:Mn QDs prepared from the precursor solution with a pH of 9 is broad. Zhang *et al.* demonstrated that interparticle electrostatic repulsion greatly affects the agglomeration growth of aqueous QDs in the initial state and that they depend on the pH of the precursor solutions [46]. It is noted that although the size distribution of QDs becomes broad, it is necessary to prepare QD from precursor solutions in the alkaline pH range to observe Mn PL.

Next, to investigate the optimum pH value of the precursor solution, ZnSe:Mn QDs were systematically prepared from precursor solutions whose pH was varied between 5 and 11. Figures S1–S8 show the reaction time dependence of absorption and PL spectra in the ZnSe:Mn QDs prepared from the various precursor solutions with different pH values. The dependence of the maximum Mn-PL intensity in each sample on the pH of

the precursor solutions is shown in Fig. 5. Mn PL was not observed in the ZnSe:Mn QDs prepared from precursor solutions with pH values of 5 and 6. From Fig. 5, the optimum pH value of the ZnSe:Mn precursor solution was found to be 10.

Next, we discuss the dependence of the Mn-PL intensity on the Mn concentration. ZnSe:Mn QDs were prepared while varying the Mn concentration between 0.5% and 10%; here, we define the Mn concentration as the mixing ratio of Zn ions and Mn ions in the precursor solutions. The pH of the precursor solution was fixed to the optimum pH of 10. Figure 6(a) shows the PL spectra of the ZnSe:Mn QDs prepared with Mn concentrations of 1%, 2%, 3%, and 7%. It was found that the Mn-PL intensity strongly depends on the Mn concentration. Figure 6(b) shows the dependence of the Mn-PL intensity on the Mn concentration. The Mn-PL intensity reaches a maximum in the samples prepared with Mn concentrations of 1.5% and 2.0%. When the Mn concentration becomes greater, the Mn-PL intensity decreases, presumably due to concentration quenching [47].

The molar ratio of anions to cations (Se/Zn) is also an important factor in the synthesis of semiconductor QDs [39]. We synthesized ZnSe:Mn QDs under various conditions while changing the Se/Zn molar ratio in the range of 0.1–0.6, where the Mn concentration was fixed at 2%. Figure 7 shows the Se/Zn molar ratio dependence of the Mn-PL intensity. It is obvious that the Se/Zn molar ratio has a large influence on the PL intensity. As the Se/Zn molar ratio becomes greater than 0.2, the PL intensity decreases drastically. From the results discussed above, the optimum conditions for the preparation of the precursor solutions of ZnSe:Mn QDs were found to be an Se/Zn molar ratio of 0.2, an Mn concentration of 2%, and a pH of 10. The maximum PL QY of the obtained ZnSe:Mn QDs was 20%. To the best of our knowledge, this QY is the highest value ever reported for a water-soluble ZnSe:Mn core QD.

The XRD pattern of the ZnSe:Mn QDs prepared with the optimum conditions is shown in Fig. 8(a). Three diffraction peaks at  $28.6^\circ$ ,  $47.8^\circ$ , and  $55.8^\circ$  corresponding to the (111), (220), and (311) lattice planes of the cubic zinc blende structure of ZnSe (JCPDS Card No. 80-0021) were observed. Figure 8(b) shows a typical TEM image of the ZnSe:Mn QDs. The growth of spherical particles with a mean diameter of 3.2 nm can be confirmed from the TEM image.

To further improve the PL QY, ZnSe:Mn/ZnS core shell QDs were prepared. It is well known that the formation of a shell layer on core QDs suppresses the nonradiative recombination rate, and an improvement in the PL QY can be expected. Figures 9(a) and 9(b) show the absorption and PL spectra of the ZnSe:Mn and ZnSe:Mn/ZnS QDs, respectively. In the ZnSe:Mn/ZnS QDs, an additional absorption structure is observed at  $\sim 4.3$  eV, which is higher than the band-gap energy of  $\sim 3.7$  eV in a ZnS bulk crystal. This transition is due to the higher excited state of the electrons and holes spreading throughout the core/shell QD [48,49].

Figures 10(a), 10(b), and 10(c) show the Zn 2p, Se 3d, and Se 3p XPS spectra, respectively, of the ZnSe:Mn core QDs. The signals observed at 1024 eV and 1048 eV correspond to those of Zn  $2p_{3/2}$  and Zn  $2p_{1/2}$ , respectively [47]. In addition, the signals observed at 51.7 eV, 158 eV, and 164 eV correspond to those of Se  $3d_{5/2}$ , Se  $3p_{3/2}$ , and Se  $3p_{1/2}$ , respectively [50]. The results of the XPS measurements for Zn 2p, Se 3d, and S 2p for the ZnSe:Mn/ZnS core/shell QDs are shown in Figs. 10(d), 10(e), and 10(f), respectively. For Zn 2p, similar XPS spectra are observed in the ZnSe:Mn core and ZnSe:Mn/ZnS core/shell QDs. Conversely, a large change in the signal intensity of Se is observed. In ZnSe:Mn/ZnS core/shell QDs, the signal intensity of Se 3d greatly decreases and the signal of S 2p is clearly observed. These results clearly demonstrate the growth of the ZnS shell on the surface of the ZnSe:Mn core QDs.

From Fig. 9(b), it is obvious that the PL properties were improved by preparing core/shell QDs. In ref. [51], Li *et al.* reported that the intensity ratio of BE-PL and Mn PL strongly depends on potential structures in type-I ZnSe:Mn/ZnS and quasi type II ZnSe:Mn/CdS/ZnS nanowires. Therefore, a further improvement of PL properties in ZnSe:Mn QDs can be expected by controlling shell material and shell thickness. It is recognized that the PL band with a peak at 2.6 eV is still observed after the ZnS shell coating. It might be attributed to a defect-related PL from ZnSe QDs containing no Mn<sup>2+</sup> ions. The growth of inorganic shells usually reduces defect-related PL intensity because the nonradiative recombination processes at the surface of core QDs are suppressed by the growth of the shells. However, the defect-related PL was still clearly observed even after the growth of the ZnS shell. One possible explanation is that the origin of the defect-related PL in the present QDs is not a surface defect but might be an internal defect. In the case of a defect-related PL caused by an internal defect, it is considered that the PL intensity does not decrease even if the nonradiative recombination processes at the surface of core QDs are suppressed by the formation of the ZnS Shell.

The PL QY of ZnSe:Mn/ZnS QDs was improved to ~30%. In ref. [52], Zhao *et al.* successfully synthesized mercaptopropionic acid-capped ZnSe:Mn/ZnO QDs with a PL QY of 31%, which is the highest value reported for Mn-doped QDs prepared via an aqueous route. The PL QY of the NAC-capped ZnSe:Mn/ZnS QDs prepared in the present study is therefore nearly the same as the current maximum value.

#### IV. CONCLUSIONS

We investigated the synthesis conditions for water-soluble NAC-capped ZnSe:Mn QDs using a hydrothermal method. The optimum conditions for the preparation of the precursor solutions were found to be a Se/Zn molar ratio of 0.2, a Mn concentration of

2%, and a pH of 10. The PL QY of the obtained ZnSe:Mn QDs reached 20%, which is the highest value ever reported for a water-soluble ZnSe:Mn core QD. Further, the PL QY was increased to 30% by preparing ZnSe:Mn/ZnS core/shell QDs.

#### SUPPLEMENTARY MATERIAL

See supplementary material for the reaction time dependence of absorption and PL spectra in ZnSe:Mn QDs prepared using precursor solutions with different pH values and for XRD patterns of ZnSe and ZnSe:Mn QDs prepared from the precursor solutions with pH = 6 and 9, respectively.

#### ACKNOWLEDGEMENTS

N.S. and D.K. acknowledges a Grant-in-Aid for Scientific Research (B) (No. 17H03538) from the Japan Society for the Promotion of Science (KAKENHI).

## References

- [1] B. O' Regan and M. Grätzel, *Nature* **353**, 737 (1991).
- [2] M. J. Currie, J. K. Mapel, T. D. Heidel, S. Goffri, and M. A. Baldo, *Science* **321**, 226 (2008).
- [3] E. Klampaftis, D. Ross, K. R. McIntosh, and B. S. Richards, *Sol. Energy Mater. Sol. Cells* **93**, 1182 (2009).
- [4] E. Klampaftis, and B. S. Richards, *Progress in Photovoltaics* **19**, 345 (2010).
- [5] L. Danos, T. Parel, T. Markvart, V. Barrioz, W. S. M. Brooks, and S. J. C. Irvine, *Solar Energy Materials and Solar Cells* **98**, 486 (2012).
- [6] H. J. Hovel, R. T. Hodgson, and J. M. Woodall, *Solar Energy Materials* **2**, 19 (1979).
- [7] A. Kojima, K. Teshima, Y. Shirai, and T. Miyasaka, *J. Am. Chem. Soc.* **131**, 6050 (2009).
- [8] Y. Iso, S. Takeshita, and T. Isobe, *J. Electrochem. Soc.* **159**, 72 (2012).
- [9] S.-W. Beak, J. -H. Shim, and J. -G. Park, *Phys. Chem. Chem. Phys.* **16**, 18205 (2014).
- [10] U. Resch- Genger, M. Grabolle, S. Cavaliere- Jaricot, R. Nitschke, and T. Nann, *Nature Methods* **5**, 763 (2008).
- [11] J. Zhou, Y. Yang, and C.-Y. Zhang, *Chem. Rev.* **115**, 11669 (2015).
- [12] L. Brus, *Appl. Phys. A* **53**, 465 (1991).
- [13] Y. Kayanuma, *Phys. Rev. B* **38**, 9797 (1988).
- [14] C. B. Murray, D. J. Norris, and M. G. Bawendi, *J. Am. Chem. Soc.* **115**, 8706 (1993).
- [15] Al. L. Efros, M. Rosen, M. Kuno, M. Nirmal, D. J. Norris, and M. G. Bawendi, *Phys. Rev. B* **54**, 4843 (1996).
- [16] V. I. Klimov, *J. Phys. Chem. B* **104**, 6112 (2000).
- [17] C. M. Donegá, M. Bode, and A. Meijerink, *Phys. Rev. B* **74**, 085320 (2006).
- [18] N. Gaponik, D. V. Talapin, A. L. Rogach, K. Hoppe, E. V. Shevchenko, A. Kornowski,

- A. Eychmüller, and H. Weller, *J. Phys. Chem. B* **106**, 7177 (2002).
- [19] A. L. Rogach, T. Franzl, T. A. Klar, J. Feldmann, N. Gaponik, V. Lesnyak, A. Shavel, A. Eychmüller, Y. P. Rakovich, and J. F. Donegan, *J. Phys. Chem. C* **111**, 14628 (2007).
- [20] D. Zhao, Z. He, W. H. Chan, and M. M. F. Cho, *J. Phys. Chem. C* **113**, 1293 (2009).
- [21] H. Bu, H. Kikunaga, K. Shimura, K. Takahashi, T. Taniguchi, and D. Kim, *Phys. Chem. Chem. Phys.* **15**, 2903 (2013).
- [22] W. Song and H. Yang, *Chem. Mater.* **24**, 1961 (2012).
- [23] R. Xie, M. Rutherford, and X. Peng, *J. Am. Chem. Soc.* **131**, 5691 (2009).
- [24] W. Xiang, C. Xie, J. Wang, J. Zhong, X. Liang, H. Yang, L. Luo, and Z. Chen, *J. Alloy. Comp.* **588**, 114 (2012).
- [25] T. Kameyama, T. Takahashi, T. Machida, Y. Kamiya, T. Yamamoto, S. Kuwabata, and T. Torimoto, *J. Phys. Chem. C* **119**, 24740 (2015).
- [26] M. A. Hines and P. G.-Sionnest, *J. Phys. Chem. B* **102**, 3655 (1998).
- [27] P. D. Cozzoli, L. Manna, M. L. Curri, S. Kudera, C. Giannini, M. Striccoli, and A. Agostiano, *Chem. Mater.* **17**, 1296 (2005).
- [28] D. Zhao, J.-T. Li, F. Gao, C. Zhang, and Z. He, *RSC Adv.* **4**, 47005 (2013).
- [29] R. N. Bhargava, D. Gallagher, X. Hong, and A. Nurmikko, *Phys. Rev. Lett.* **72**, 416 (1994).
- [30] C. Gan, Y. Zhang, D. Battaglia, X. Peng, and M. Xiao, *Appl. Phys. Lett.* **92**, 241111 (2008).
- [31] R. Zeng, T. Zhang, G. Dai, and B. Zou, *J. Phys. Chem. C* **115**, 3005 (2011).
- [32] Y. He, H.-F. Wang, and X.-P. Yan, *Anal. Chem.* **80**, 3832 (2008).
- [33] K. Manzoor, S. Johny, D. Thomas, S. Setua, D. Menon, and S. Nair, *Nanotechnology* **20**, 065102 (2009).
- [34] D. Gerion, F. Pinaud, S. C. Williams, W. J. Parak, D. Zanchet, S. Weiss, and A. P.

- Alivisatos, J. Phys. Chem. B **105**, 8861 (2001).
- [35] T. Zhang, J. Ge, Y. Hu, and Y. Yin, Nano Lett. **7**, 3203 (2007).
- [36] A. Aboulaich, M. Geszke, L. Balan, J. Ghanbaja, G. Medjahdi, and R. Schneider, Inorg. Chem. **49**, 10940 (2010).
- [37] M. Hardzei and M. Artemyev, J. Lumin. **132**, 425 (2012).
- [38] T. Watanabe, K. Takahashi, K. Shimura, H. Bu, H.-D. Kim, and D. Kim, Bull. Chem. Soc. Jpn. **90**, 52 (2017).
- [39] Y-S. Lee, K. Nakano, H-B. Bu, and D. Kim, Appl. Phys. Express **10**, 065001 (2017).
- [40] D. Kim, S. Okahara, M. Nakayama, and Y. Shim, Phys. Rev. B **78**, 153301 (2008).
- [41] D. Kim, H. Yokota, T. Taniguchi, and M. Nakayama, J. Appl. Phys. **114**, 154307 (2013).
- [42] Y-S. Lee, H. Bu, T. Taniguchi, T. Takagi, S. Sobue, H. Yamada, T. Iwaki, and D. Kim, Chem. Lett. **45**, 878 (2016).
- [43] A. A. Bol and A. Meijerink, Phys. Rev. B **58**, R15997 (1998).
- [44] W. Chena, R. Sammynaiken, Y. Huangb, J. Malm, R. Wallenberg, J. Bovinc, and N. A. Kotov, J. Appl. Phys. **89**, 1120 (2001).
- [45] D. Kim, M. Miyamoto, and M. Nakayama, J. Appl. Phys. **100**, 094313 (2006).
- [46] H. Zhang, Y. Liu, J. Zhang, C. Wang, M. Li, and B. Yang, J. Phys. Chem. C **112**, 1885 (2008).
- [47] M. Geszke, M. Murias, L. Balan, G. Medjahdi, J. Korczynski, M. Moritz, J. Lulek, and R. Schneider, Acta Biomater. **7**, 1327 (2011).
- [48] N. Razgoniaeva, P. Moroz, M. Yang, D. S. Budkina, H. Eckard, M. Augspurger, D. Khon, A. N. Tarnovsky, and M. Zamkov, J. Am. Chem. Soc. **139**, 7815 (2017).
- [49] T. Watanabe, K. Takahashi, K. Shimura, and D. Kim, Phys. Rev. B **96**, 035305 (2017).
- [50] J. F. Moulder, W. F. Stickle, P. E. Sobol, and K. D. Bomben, edited by J. Chastain,

*Handbook of X-ray Photoelectron Spectroscopy* (Physical Electronics, Minnesota, 1995).

[51] Z. Li, E. Hofman, A. Blaker, A. H. Davis, B. Dzikovski, D.-K. Ma, and W. Zheng, *ACS Nano* **11**, 12591 (2017).

[52] B. Zhao, Y. Yao, K. Yang, P. Rong, P. Huang, K. Sun, X. An, Z. Li, X. Chen, and W. Li, *Nanoscale* **6**, 12345 (2014).

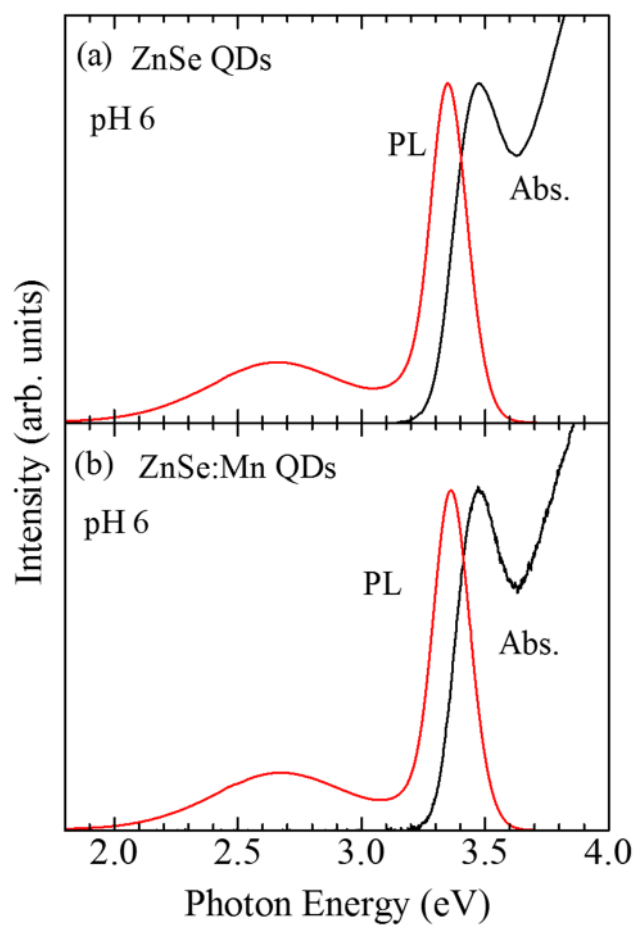


FIG. 1. Absorption and PL spectra of (a) ZnSe and (b) ZnSe:Mn QDs prepared with a reaction time of 30 min using a precursor solution with a pH of 6.

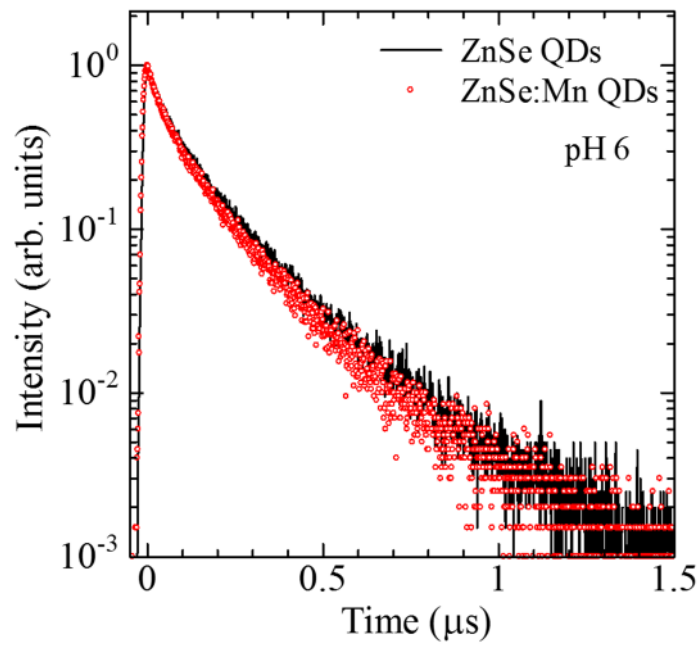


FIG. 2. PL-decay profiles detected at 2.68 eV in ZnSe and ZnSe:Mn QDs prepared with a reaction time of 30 min using a precursor solution with a pH of 6.

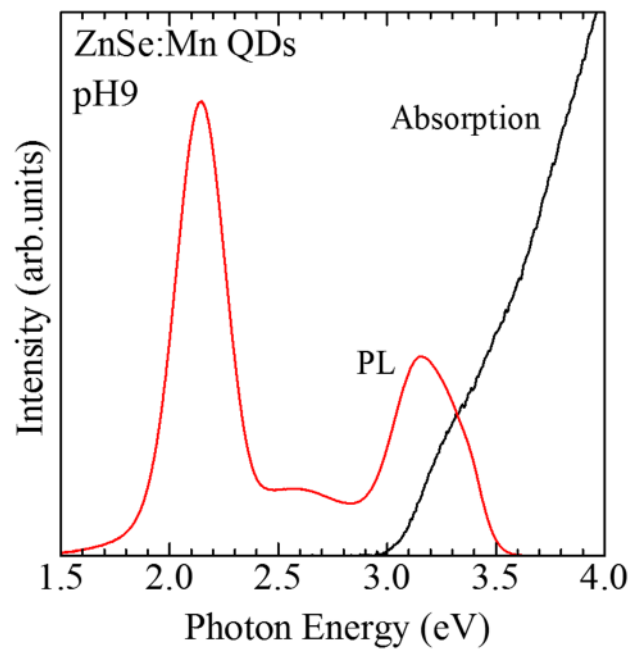


FIG. 3. Absorption and PL spectra of ZnSe:Mn QDs prepared from a ZnSe:Mn (2% Mn) precursor solution with a pH of 9.

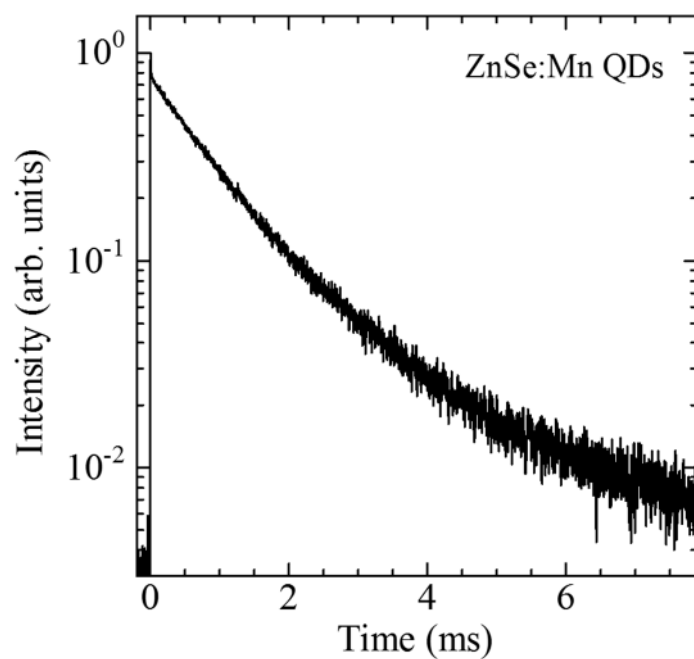


FIG. 4. PL-decay profile detected at the PL peak of 2.1 eV in ZnSe:Mn QDs prepared from a ZnSe:Mn (2% Mn) precursor solution with a pH of 9.

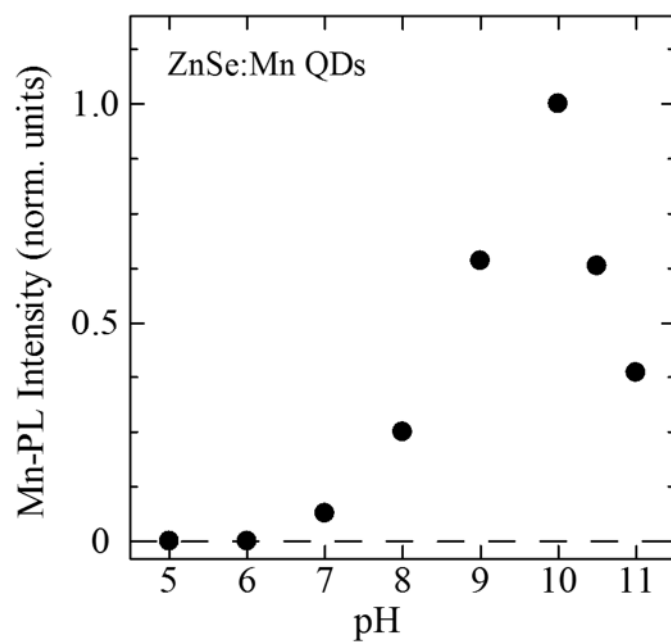


FIG. 5. The dependence on the pH of the precursor solutions of the maximum PL intensity of Mn PL in each sample.

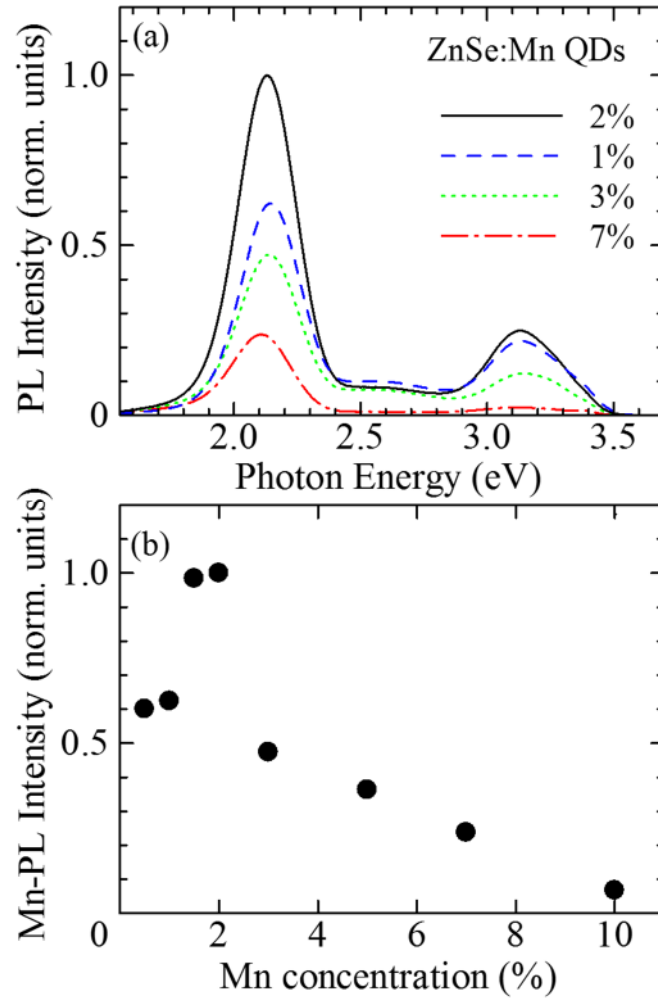


FIG. 6. (a) PL spectra of ZnSe:Mn QDs prepared with Mn concentrations of 1%, 2%, 3%, and 7%. (b) The dependence of the Mn-PL intensity on the Mn concentration.

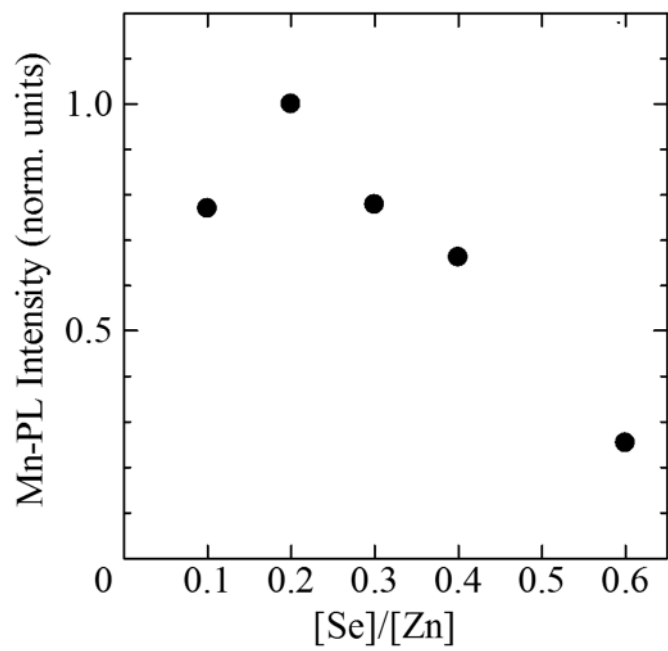


FIG. 7. The Se/Zn molar ratio dependence of the Mn-PL intensity.

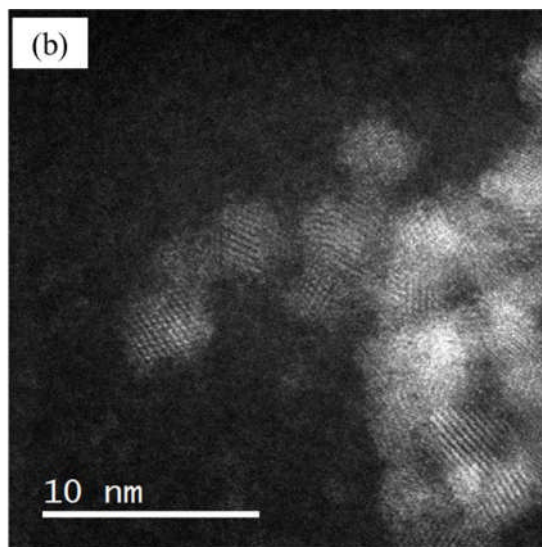
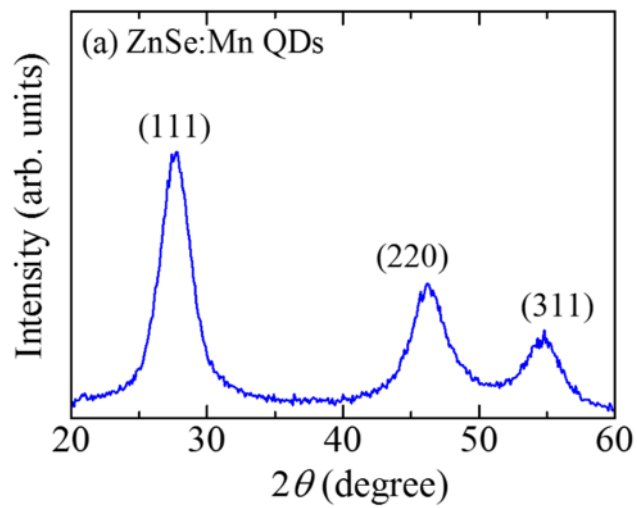


FIG. 8. (a) XRD pattern and (b) Typical TEM image of ZnSe:Mn QDs prepared with the optimum conditions.

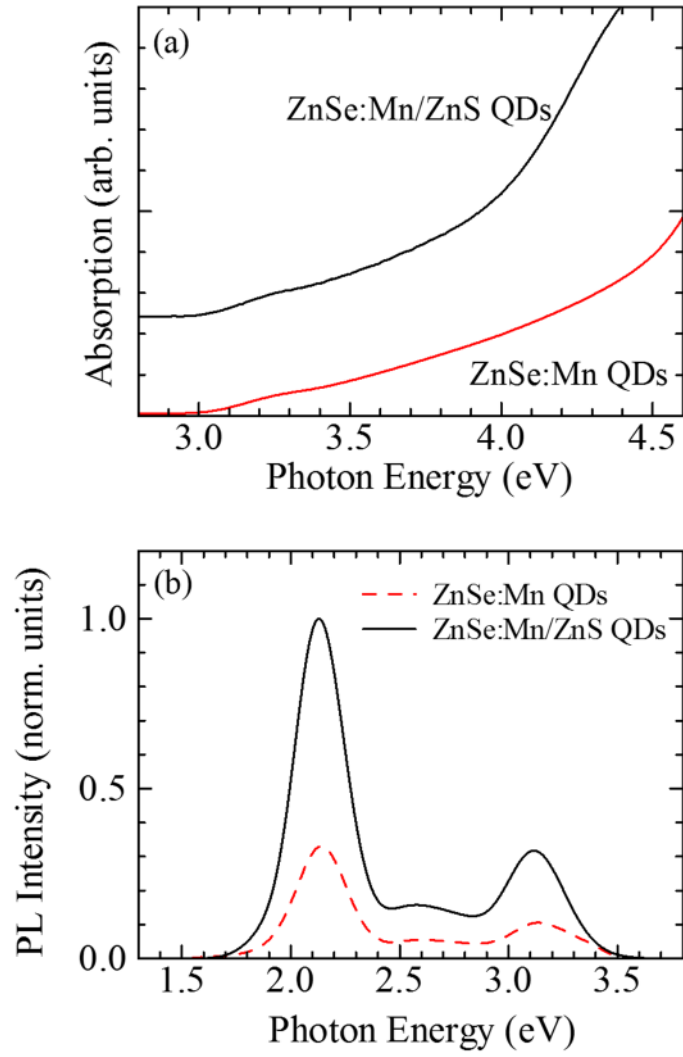


FIG. 9. (a) Absorption and (b) PL spectra of ZnSe:Mn and ZnSe:Mn/ZnS QDs.

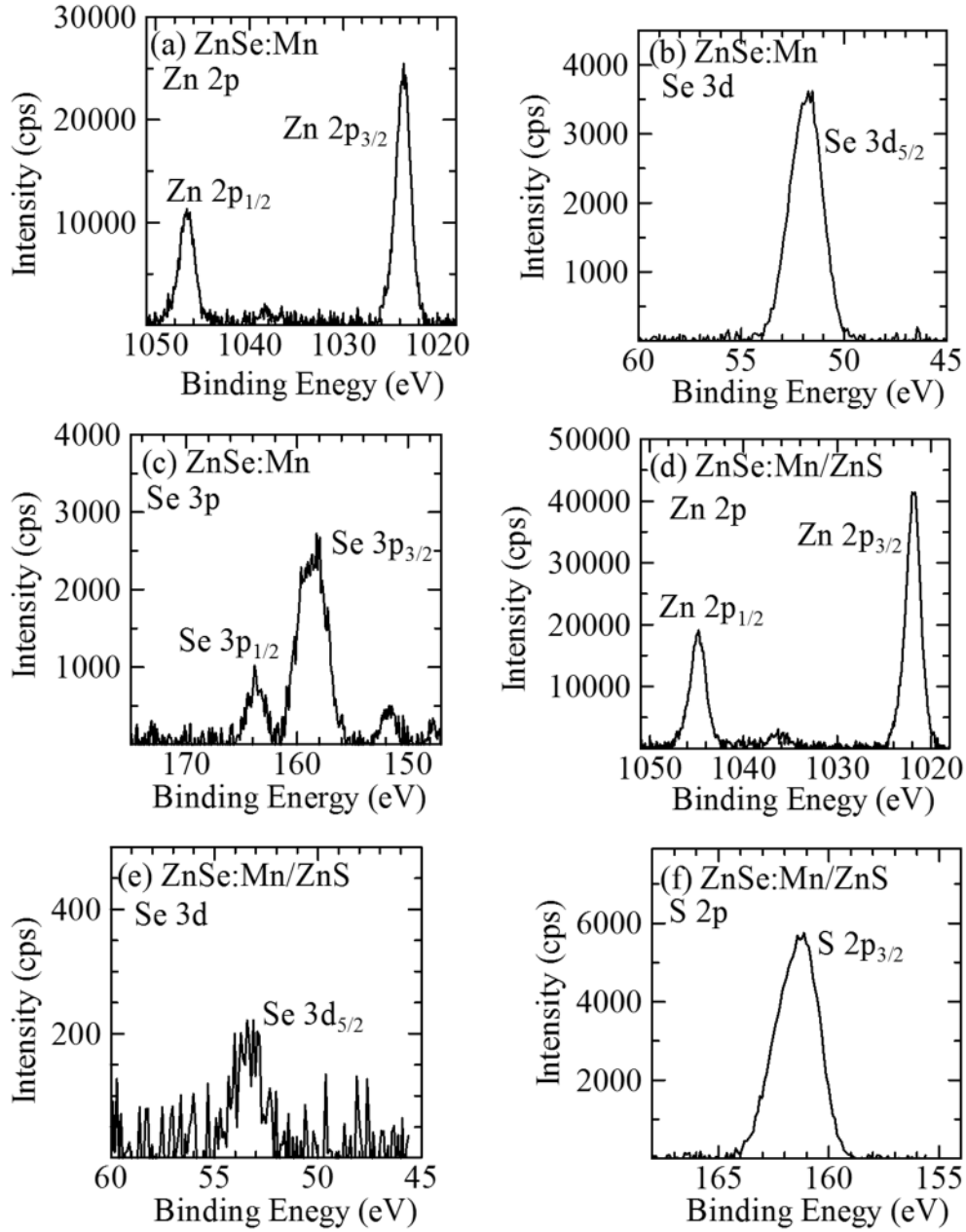


FIG. 10. XPS spectra for (a) Zn 2p, (b) Se 3d, and (c) Se 3p of ZnSe:Mn core QDs and for (d) Zn 2p, (e) Se 3d, and (f) S 2p of ZnSe:Mn/ZnS core/shell QDs.